

# Change in Reaction Pathway in the Reduction of 3,5-Di-*tert*-butyl-1,2-benzoquinone with Increasing Concentrations of 2,2,2-Trifluoroethanol

Norma A. Macías-Ruvalcaba, Noriko Okumura, and Dennis H. Evans\*

Department of Chemistry, University of Arizona, Tucson, Arizona 85721

Received: June 26, 2006; In Final Form: August 15, 2006

The electrochemical reduction of 3,5-di-*tert*-butyl-1,2-benzoquinone, **1**, has been studied in acetonitrile with added 2,2,2-trifluoroethanol, **2**. At low concentrations of **2** the reaction proceeds by the following pathway: reduction of the quinone (Q) to its anion radical (Q<sup>•−</sup>) followed by complexation of the anion radical with **2** (HA) and the further reduction of the hydrogen-bonded complex (Q<sup>•−</sup>(HA)) to form HQ<sup>•−</sup> and A<sup>−</sup>. The latter reaction is a concerted proton and electron-transfer reaction (CPET). At higher concentrations of **2**, the pathway changes. The first steps remain the same, but now Q<sup>•−</sup>(HA) is reduced to HQ<sup>•−</sup> via a disproportionation reaction with Q<sup>•−</sup> along with proton transfer from HA to Q<sup>•−</sup> to form HQ<sup>•</sup> which is reduced to HQ<sup>•−</sup>. The only mechanism that could be found which would account for all of the data involves proton transfer to Q<sup>•−</sup> occurring within a higher complex, Q<sup>•−</sup>(HA)<sub>3</sub>.

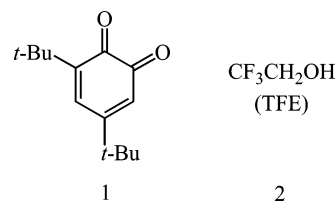
## 1. Introduction

The reduction of quinones is important in many areas including biology, chemical technology, sensor applications, and energy conversion. Hydrogen bonding and proton transfer are of key importance in controlling the reduction potential and the reaction path.<sup>1,2</sup> Numerous studies have shown that both intramolecular hydrogen bonding and intermolecular hydrogen bonding, by way of added hydrogen-bond donors, can affect the first stage of reduction, neutral quinone (Q) to anion radical (Q<sup>•−</sup>), reaction 1, primarily through interaction with the anion radical (reaction 3).<sup>3</sup> The effects on the second stage, Q<sup>•−</sup> to dianion (Q<sup>2−</sup>), reaction 2, are more pronounced than the first, due to stronger hydrogen-bonding interactions with the dianion (reaction 4) as compared to the anion radical. Here, HA represents the hydrogen-bond donor and only 1:1 complexes are shown, though it is frequently necessary to invoke higher complexes.

For hydrogen-bond donors that are relatively strong acids, the proton can participate in the reaction by protonating the anion radical to form a neutral radical, HQ<sup>•</sup>, reaction 5. HQ<sup>•</sup> is more easily reduced than the original quinone, resulting in the formation of the two-electron product, HQ<sup>•−</sup>, the anion arising from deprotonation of the hydroquinone. The signature of this

behavior is that the first reduction peak increases in magnitude as HA is added due to the sequence of reactions 1, 5, and 6. If reaction 5 is sufficiently fast, the first peak becomes irreversible, and its height approaches that of a two-electron process. Another reaction, disproportionation reaction 7, will also cause an increase in height of the first reduction peak.

Exceptional behavior was found for 3,5-di-*tert*-butyl-1,2-benzoquinone, **1**, when studied in acetonitrile in the presence of water.<sup>4</sup> Here the anion radical forms a 1:1



hydrogen-bonded complex with water (reaction 3). Water is not a strong enough acid to allow proton transfer to occur (reaction 5) even at concentrations as high as 1 M, and the disproportionation (reaction 7) is too slow to affect the voltammetry. Rather, the hydrogen-bonded water–anion radical complex is the reactant in the second stage of reduction, a process that produces an irreversible drawn-out voltammetric peak whose potential moves in the positive direction as the concentration of water is increased. This reaction, reaction 8, is a concerted proton and electron transfer (CPET) in which electron transfer from the electrode to the complex is concerted with proton transfer within the complex from water to the quinone moiety. CPET reactions have also been seen for electrochemical reduction of superoxide,<sup>5</sup> oxidation of an amino phenol,<sup>6</sup> and oxidation of 2,5-dicarboxylate-1,4-hydrobenzoquinone.<sup>7</sup> Arguments supporting the CPET designation, as opposed to possible two-step pathways, have been fully developed for each case.<sup>4–7</sup>

In the reduction of **1**, behavior similar to the addition of water was seen when 2,2,2-trifluoroethanol, **2**, was the hydrogen-bonding additive.<sup>4</sup> However, in this case the CPET reaction appears at very low concentrations of **2**, even as low as a few millimolar. Apparently, **2** is not a sufficiently strong acid to



\* To whom correspondence should be addressed. E-mail: dhevans@email.arizona.edu.

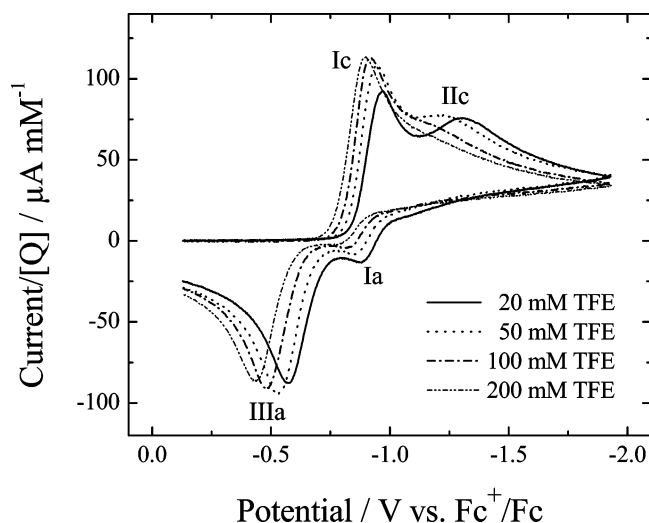


**Figure 1.** Voltammograms of 3,5-di-*tert*-butyl-1,2-benzoquinone, **1**, in the presence of various concentrations of 2,2,2-trifluoroethanol, **2** (TFE). The concentrations of **1** were close to 2 mM. The current scale has been divided by the actual concentrations of **1** to allow for visual comparison of peak heights. Scan rate: 1.00 V/s.

protonate the anion radical (reaction 5), at least at low concentrations. However, as the concentration of **2** is increased, it is possible that the proton transfer prior to electron transfer (reactions 5 and 6) may begin to compete with the CPET (reaction 8). Exploration of that possibility is the subject of the present report.

## 2. Experimental Section

**2.1. Chemicals and Reagents.** The solvent was acetonitrile, and the electrolyte was tetrabutylammonium hexafluorophosphate ( $\text{Bu}_4\text{NPF}_6$ ). Sources and treatment of solvent and electrolyte have been described.<sup>8</sup> 3,5-Di-*tert*-butyl-1,2-benzoquinone, **1**, was obtained from Aldrich and recrystallized twice from ethanol. 2,2,2-Trifluoroethanol, **2**, was obtained from Aldrich and used as received.

**2.2. Electrochemical Cells, Electrodes, and Instrumentation.** These were as described earlier.<sup>8</sup> The working electrode was a 0.3-cm diameter glassy carbon electrode whose area was determined to be 0.0814  $\text{cm}^2$ . The reference electrode was a silver wire immersed in 0.10 M  $\text{Bu}_4\text{NPF}_6$ /0.010 M  $\text{AgNO}_3$  in acetonitrile. The potential of this reference electrode was periodically measured with respect to the reversible ferrocene/ferrocenium potential, and all potentials reported in this work are with respect to ferrocene. The temperature of the cell was maintained at 298 K. Voltammograms with supporting electrolyte and **2** alone (without **1**) were recorded and subtracted from the voltammograms of **1** to obtain background-corrected data.

**2.3. Calculations.** Digital simulations were conducted DigiElch, version 2.0, a free software package for the Digital simulation of common Electrochemical experiments (<http://www.digielch.de>).<sup>9</sup>

Complete geometry optimization and frequency calculations were performed according to the density functional theory (DFT) using the B3LYP/3-21g level with the Gaussian 03 program.<sup>10</sup> For radicals, the corresponding unrestricted (UB3LYP) method was used. Solvation energies were computed using the polarizable continuum model (PCM).

## 3. Results and Discussion

Figure 1 shows the effect of increasing concentrations of 2,2,2-trifluoroethanol (**2**) on the voltammetry of 3,5-di-*tert*-butyl-

1,2-benzoquinone (**1**). Several features are apparent in the voltammograms. The second, irreversible reduction peak, IIC, which is fully developed with only 1 mM added **2**,<sup>4</sup> moves in the positive direction with increasing concentrations of **2** and decreases in height until it is almost absent at 100 mM **2**. Meanwhile, the first reduction peak, Ic, also shifts in the positive direction and, at high enough concentrations of **2**, begins to increase in height. It is this increase that signals the transition in mechanism from CPET (reactions 1, 3 and 8) to proton transfer preceding electron transfer (reactions 1, 3, 5 and 6; we shall see, however, that this simple sequence cannot account for the data). Also apparent in the figure are small anodic peaks for oxidation of the anion radicals (Ia) and a major oxidation peak, IIIa, that is due to oxidation of  $\text{HQ}^-$ , reverse of reaction 6.

We first analyzed the shift in the first reduction peak in terms of the formation of hydrogen-bonded complexes between **2** and the anion radical, reactions 3, 9, and 10.



Voltammograms encompassing only the first set of peaks (Ic and Ia) were recorded for scan rates between 10 and 50 V/s and concentrations of **2** between 2 and 50 mM. Lower scan rates and higher concentrations of **2** were avoided in order to eliminate reactions leading to the two-electron product, disproportionation (reaction 7), or proton transfer preceding electron transfer. The analysis was based on digital simulation of the curves with equal diffusion coefficients for all quinone species ( $1.5 \times 10^{-5} \text{ cm}^2/\text{s}$ ) adjusted to match the cathodic peak height. The diffusion coefficient of **2** was set at  $2.8 \times 10^{-5} \text{ cm}^2/\text{s}$ . The value of  $E^\circ_1$ ,  $-0.960 \text{ V}$ , was obtained by fitting the voltammogram with no added **2**. The complexation reactions were treated as fast and reversible processes, leaving only the formation constants as adjustable parameters in fitting the voltammograms with added **2**. It was found that only the 1:1 and the 2:1 complexes needed to be considered. The best fit for all of the data was  $K_3 = 143 \text{ M}^{-1}$  and  $K_9 = 42 \text{ M}^{-1}$ . In this way, values of  $E^\circ_1$ ,  $K_3$ , and  $K_9$  were obtained, and these were held constant as the analysis was extended to wider potential scan ranges that encompassed all peaks, Ic, IIC, Ia, and IIIa (Figure 1).

Data were obtained for scan rates of 0.1, 0.2, 0.3, 0.5, 1, 2, 3, 5, 10, 20, and 30 V/s for 2.0 mM **1** and 0.020, 0.050, 0.100, and 0.200 M **2**. Results for the same scan rates were also obtained at 0.100 M **2** and 0.50 and 5.0 mM **1**. The focus of the analysis will be to account for the growth of peak Ic with increases in the concentration of **2**. At lower concentrations and moderate scan rates, peak Ic corresponds to the one-electron reduction of the quinone with no contribution by reactions leading to the two-electron product. This was confirmed by simulation of the voltammogram of 2.0 mM **1**, 0.020 M **2** at 1.0 V/s, where the height of Ic was fit exactly by the parameters (see above) used to simulate the Ic/Ia set of peaks (reactions 1, 3, 9, and 10). So, under these conditions the only pathway open to the two-electron product is by the reduction of the  $\text{Q}^{\bullet-}(\text{HA})$  complex at the electrode (peak IIC), reaction 8.

Simulation of the full scans started with the parameter values obtained by simulation of the scans confined to peaks Ic and Ia, viz.  $E^\circ_1 = -0.960 \text{ V}$ ,  $K_3 = 143 \text{ M}^{-1}$ , and  $K_9 = 42 \text{ M}^{-1}$ . The reaction giving rise to the irreversible reduction of the 1:1 complex according to reaction 8 with  $E^\circ_8$

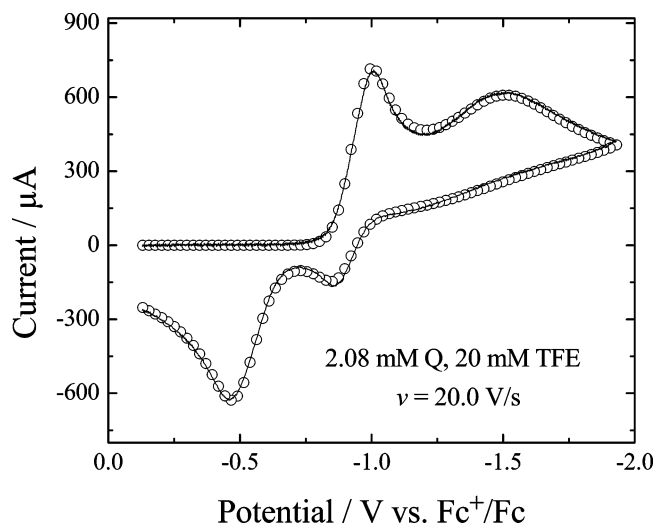
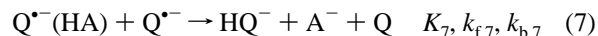


**Figure 2.** Cyclic voltammogram of 2.08 mM **1** in the presence of 0.020 M **2** (TFE) at 20.0 V/s. Full curve: background-corrected experimental voltammogram. Symbols: simulation. Key simulation parameters:  $K_3 = 143 \text{ M}^{-1}$ ,  $K_9 = 42 \text{ M}^{-1}$ ,  $K_{10} = 0.10 \text{ M}^{-1}$  with all hydrogen-bond reactions considered to be fast.  $k_{f,7} = 1000 \text{ M}^{-1} \text{ s}^{-1}$ ;  $k_{f,15} = 3000 \text{ s}^{-1}$ . For other simulation parameters see Supporting Information, Table S1.

$= -0.47 \text{ V}$  as estimated earlier.<sup>4</sup> The electron-transfer coefficient,  $\alpha_8$ , was adjusted to 0.2 to account for the drawn-out appearance of IIc. Finally,  $k_{s,8}$  was adjusted for the 0.020 M **2** data set in order to achieve the correct position of peak IIc. This value,  $5.8 \times 10^{-5} \text{ cm/s}$ , was maintained constant, and  $E^\circ_8$  was adjusted about 0.3 V in the positive direction on increasing the concentration of **2** from 0.020 to 0.200 M. It was deemed that  $k_{s,8}$  should be constant as it refers to a particular reaction, reaction 8, which does not change with the concentration of **2**. By contrast,  $E^\circ_8$  is expected to move in the positive direction due to the fact that **2** is a reactant and that **2** will stabilize both products,  $\text{HQ}^-$  and  $\text{A}^-$ , through hydrogen bonding as the concentration of **2** is increased. Similar arguments have been advanced in the case of CPET in the reduction of superoxide.<sup>5b</sup> Peak IIIa was treated as the irreversible, two-electron oxidation of  $\text{HQ}^-$  and  $\text{A}^-$  to **Q** and **HA**. The potentials for the two steps of oxidation were allowed to shift in the positive direction to account for the shift seen as the concentration of **2** was increased.

What reaction pathway will account for the increase in peak Ic as the concentration of **2** is increased? In what follows, we will describe the sequence of reasoning and testing through which a satisfactory mechanism was developed. Examples of the end result are shown in Figures 2–5 which compare simulations with experiment for different scan rates and concentrations of **2**. Tables of simulation parameters and more comparisons of simulations with experimental voltammograms are presented in the Supporting Information.

The simplest mechanism that would account for the growth in peak Ic as the concentration of **2** was increased would be disproportionation reaction 7. This reaction is highly favored,



and its equilibrium constant was calculated from the  $\text{p}K_a$  of  $\text{HQ}^-$ ,  $\text{p}K_a$  of **2**, and  $E^\circ_2$  using estimates discussed earlier.<sup>4</sup> The result was  $K_7 = 2 \times 10^8 \text{ M}$ , attesting to the total irreversibility of reaction 7. This reaction occurs with water as the hydrogen-bond donor, but it is too slow to affect the voltammetry, and in fact, the slow disappearance of the anion radical in the presence

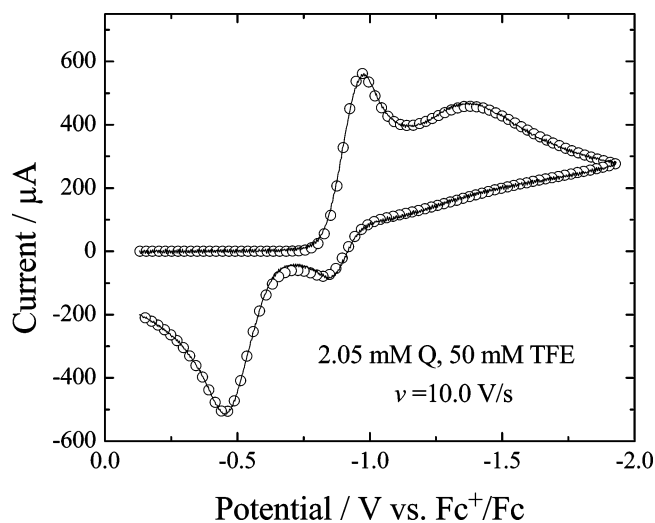


**Figure 3.** Cyclic voltammogram of 2.05 mM **1** in the presence of 0.050 M **2** (TFE) at 10.0 V/s. Full curve: background-corrected experimental voltammogram. Symbols: simulation. Key simulation parameters same as in Figure 2.

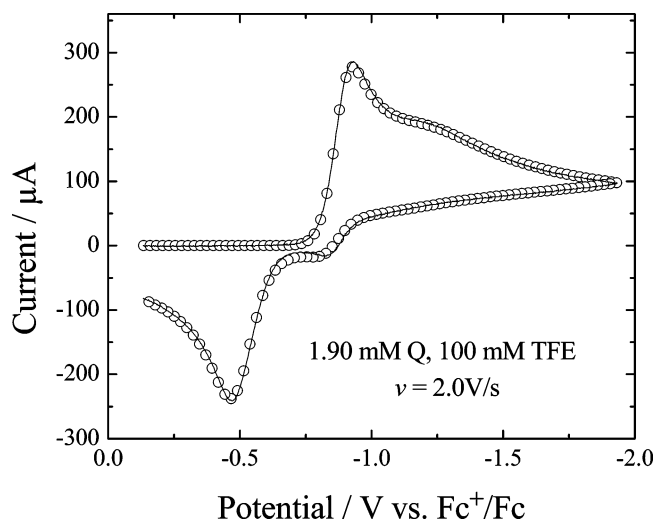
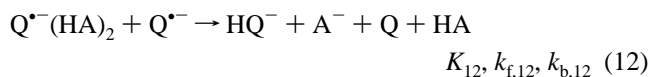
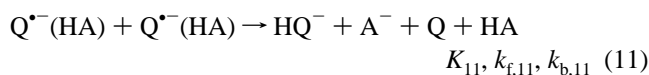


**Figure 4.** Cyclic voltammogram of 1.90 mM **1** in the presence of 0.100 M **2** (TFE) at 2.0 V/s. Full curve: background-corrected experimental voltammogram. Symbols: simulation. Key simulation parameters same as in Figure 2.

of water could be monitored by recording voltammograms as a function of elapsed time.<sup>4</sup> We find that reaction 7 or a related reaction is much faster when **2** is used. The green color of 1.6 mM  $\text{Q}^{\bullet-}$ , prepared by controlled potential electrolysis, disappeared within the mixing time upon addition of sufficient **2** to make its final concentration 66 mM.

Introduction of reaction 7 into the simulation allowed quite acceptable agreement to be obtained at all scan rates and all concentrations of **2**. The only difficulty was that it was necessary to make large increases in the value of  $k_{f,7}$  as the concentration of **2** increased. This nonconstant rate constant signifies that this simple reaction scheme is inadequate.

Two other disproportionation reactions were tested, reactions 11 and 12.



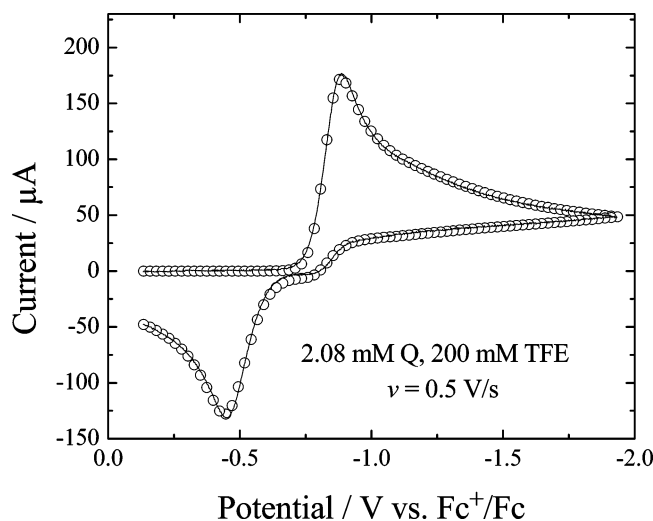


**Figure 5.** Cyclic voltammogram of 2.08 mM **1** in the presence of 0.200 M **2** (TFE) at 0.50 V/s. Full curve: background-corrected experimental voltammogram. Symbols: simulation. Key simulation parameters same as in Figure 2.

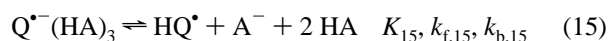
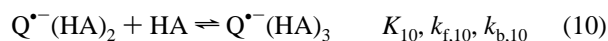
Neither of these reactions allowed fitting the data for all concentrations of **2** without using increasing values of the forward rate constant with increasing concentrations of **2**.

Two examples of proton transfer preceding electron transfer were also tested with similar results (reactions 13 and 14 each followed by reaction 6).



The result was the same: increased values of the forward rate constants of reactions 13 and 14 with increasing concentration of **2** were needed to fit all of the data.

As reactions such as 7 undoubtedly occur as evidenced by the rapid discharge of the color of  $Q^{\bullet-}$  upon addition of **2** (see above), combinations of reaction 7 with 13 or 14 were attempted, but the trend was unchanged: increasing rate constants with increasing concentration of **2**. What is needed, it would appear, is the introduction of a minor species as reactant, a species whose concentration increases rapidly with the concentration of **2**. A possibility is the 3:1 complex (reaction 10), which is of such minor importance that the shift in peaks Ic and Ia can be adequately accounted for when it is neglected.<sup>11</sup> Proton transfer within this 3:1 complex (reaction 15)



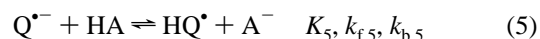
produces  $HQ^{\bullet}$  which is reduced via reaction 6. (In reactions 14 and 15, free HA is indicated as a product. It is recognized that this HA may hydrogen bond to one or both products.)

It was found that all of the data acquired at 0.020, 0.050, 0.100, and 0.200 M **2** at 2.0 mM **1**, as well as 0.100 M **2** at 0.50 and 5.0 mM **1**, could be adequately accounted for by making reactions 10 and 15 fast and reversible with  $K_{10} = 0.10 \text{ M}^{-1}$  and  $K_{15} = 0.005 \text{ M}^2$ . Best agreement was obtained with the inclusion of disproportionation reaction 7 with  $k_{f,7} = 1\,000$

$\text{M}^{-1} \text{ s}^{-1}$ . As mentioned above, this solution-phase reaction is quite rapid as judged by the disappearance of the color of the anion radical upon addition of **2**. The fact that the same simulation parameters fit data obtained over a 10-fold range of concentrations of **2** supports the inclusion of the second-order disproportionation, reaction 7.

Unlike  $K_3$  and  $K_9$ , which can be somewhat independently evaluated through analysis of peaks Ic/Ia at low concentrations of **2** and fast scan rates,  $K_{10}$  and  $K_{15}$  can only be determined from the fits to the full scans, and we suspect that other combinations of these equilibrium constants might also allow satisfactory fits to the data. The novel feature in this mechanism is the necessity of including reaction 15, internal proton transfer within the 3:1 complex. This of course is only an inference based on our ability to fit the data with this mechanism. A number of factors are ignored in this treatment. These include the self-association of **2**, formation of hydrogen-bonded complexes with species other than  $Q^{\bullet-}$ , and possible direct effects of high concentrations of **2** on the rate of reaction 7, for example (solvent effect).

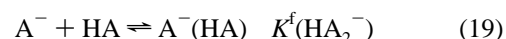
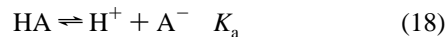
Is it reasonable to assume that proton transfer between  $Q^{\bullet-}$  and HA is strongly disfavored but will become feasible in the 3:1 complex (reaction 15)? DFT calculations (B3LYP/3-21g) along with PCM, to account for solvation by acetonitrile, were carried out for reaction 5. The energy change was found to be +26 kcal/mol so the reaction is strongly disfavored.



A factor that will favor proton transfer in the higher complexes is the stabilization of  $A^{-}$  by hydrogen bonding with HA as in reactions 16 and 17.

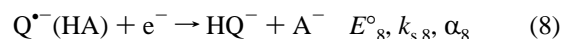


This effect is analogous to homoconjugation (reaction 19),



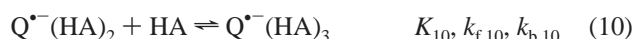
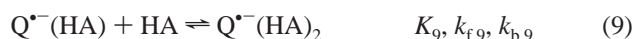
which enhances the acidity of weak acids in solvents such as acetonitrile.<sup>12</sup> Such factors, all related to hydrogen bonding, may work to make proton transfer to  $Q^{\bullet-}$  sufficiently less unfavorable to allow the reaction to proceed by way of the 3:1 complex, reaction 15.

To summarize, we have detected and characterized a change in reaction pathway in the reduction of **1** as the concentration of **2** is increased. At low concentrations of **2**, less than about 20 mM, the reaction pathway is reaction 1 followed by reaction 3 and finally the CPET reaction 8.



However, at higher concentrations of **2** there is a transition to the following reaction sequence:





This mechanism, with the inclusion of reaction 8, was found to be able to account for all of the voltammetric data at various concentrations of **1** and **2** as well as different scan rates. At the highest concentrations and lowest scan rates, the reaction proceeds exclusively by this latter pathway, and no anion radical remains to be reduced at more negative potentials where the CPET reaction occurs.

**Acknowledgment.** This research was supported by the National Science Foundation, Grant CHE 0347471.

**Supporting Information Available:** Tables of simulation parameters and additional examples of fits of simulations to the experimental voltammograms of **1** in the presence of various concentrations of **2**. This material is available free of charge via the Internet at <http://pubs.acs.org>.

## References and Notes

- (1) Chambers, J. Q. In *The Chemistry of the Quinonoid Compounds*; Patai, S., Rappaport, Z., Eds.; Wiley: New York, 1988; Vol. 2, Part 1, pp 719–757.
- (2) Aguilar-Martínez, M.; Macías-Ruvalcaba, N. A.; Bautista-Martínez, J. A.; Gómez, M.; González, F. J.; González, I. *Curr. Org. Chem.* **2004**, *8*, 1721–1738.
- (3) (a) Gupta, N.; Linschitz, H. *J. Am. Chem. Soc.* **1997**, *119*, 6384–6391. (b) Ge, Y.; Lilienthal, R. R.; Smith, D. K. *J. Am. Chem. Soc.* **1996**, *118*, 3976–3977. (c) Goulart, M. O. F.; de Abreu, F. C.; Ferraz, P. A. L.; Tonholo, J.; Glezer, V. In *Novel Trends in Electroorganic Synthesis*; Torii, S., Ed.; Springer-Verlag: Tokyo, 1998; pp 359–362. (d) Okumura, N.; Uno, B. *Bull. Chem. Soc. Jpn.* **1999**, *72*, 1213–1217. (e) Aguilar-Martínez, M.; Cuevas, G.; Jiménez-Estrada, M.; González, I.; Lotina-Hennsen, B.; Macías-Ruvalcaba, N. *J. Org. Chem.* **1999**, *64*, 3684–3694. (f) Uno, B.; Okumura, N.; Goto, M.; Kano, K. *J. Org. Chem.* **2000**, *65*, 1448–1455. (g) Ge, Y.; Smith, D. K. *Anal. Chem.* **2000**, *72*, 1860–1865. (h) Ge, Y.; Miller, L.; Ouimet, T.; Smith, D. K. *J. Org. Chem.* **2000**, *65*, 8831–8838. (i) Ferraz, P. A. L.; de Abreu, F. C.; Pinto, A. V.; Glezer, V.; Tonholo, J.; Goulart, M. O. F. *J. Electroanal. Chem.* **2001**, *507*, 275–286. (j) Aguilar-Martínez, M.; Bautista-Martínez, J. A.; Macías-Ruvalcaba, N.; González, I.; Tovar, E.; del Alizal, T. M.; Collera, O.; Cuevas, G. *J. Org. Chem.* **2001**, *66*, 8349–8363. (k) Gómez, M.; González, F. J.; González, I. *J. Electro-*

*chem. Soc.* **2003**, *150*, E527–E534. (l) Garza, J.; Vargas, R.; Gómez, M.; González, I.; González, F. J. *J. Phys. Chem. A* **2003**, *107*, 11161–11168. (m) Gómez, M.; González, I.; González, F. J.; Vargas, R.; Garza, J. *Electrochem. Commun.* **2003**, *5*, 12–15. (n) Gómez, M.; Gómez-Castro, C. Z.; Padilla-Martínez, I. I.; Martínez-Martínez, F. J.; González, F. J. *J. Electroanal. Chem.* **2004**, *567*, 269–276. (o) Macías-Ruvalcaba, N. A.; González, I.; Aguilar-Martínez, M. *J. Electrochem. Soc.* **2004**, *151*, E110–E118. (p) Okumura, N.; Evans, D. H. In *Analytical, Mechanistic and Synthetic Organic Electrochemistry. Sixth International Manuel M. Baizer Symposium in Honor of Dennis H. Evans and Masao Tokuda*; Lessard, J., Hapiot, P., Taniguchi, I., Eds.; Electrochemical Society: Pennington, NJ; PV **2004**-10, pp 21–24. (q) Gómez, M.; González, F. J.; González, I. *J. Electroanal. Chem.* **2005**, *578*, 193–202.

(4) Lehmann, M. W.; Evans, D. H. *J. Phys. Chem. B* **2001**, *105*, 8877–8884.

(5) (a) Costentin, C.; Evans, D. H.; Robert, M.; Savéant, J.-M.; Singh, P. S. *J. Am. Chem. Soc.* **2005**, *127*, 12490–12491. (b) Singh, P. S.; Evans, D. H. *J. Phys. Chem. B* **2006**, *110*, 637–644.

(6) Costentin, C.; Robert, M.; Savéant, J.-M. *J. Am. Chem. Soc.* **2006**, *128*, 4552–4553.

(7) Costentin, C.; Robert, M.; Savéant, J.-M. *J. Am. Chem. Soc.* **2006**, *128*, 8726–8727.

(8) Macías-Ruvalcaba, N. A.; Evans, D. H. *J. Phys. Chem. B* **2005**, *109*, 14642–14647.

(9) (a) Rudolph, M. *J. Electroanal. Chem.* **2003**, *543*, 23–29. (b) Rudolph, M. *J. Electroanal. Chem.* **2004**, *571*, 289–307. (c) Rudolph, M. *J. Electroanal. Chem.* **2003**, *558*, 171–176. (d) Rudolph, M. *J. Comput. Chem.* **2005**, *26*, 619–632. (e) Rudolph, M. *J. Comput. Chem.* **2005**, *26*, 633–641. (f) Rudolph, M. *J. Comput. Chem.* **2005**, *26*, 1193–1204.

(10) Frisch, M. J.; Trucks, G. W.; Schlegel, H. B.; Scuseria, G. E.; Robb, M. A.; Cheeseman, J. R.; Montgomery, J. A., Jr.; Vreven, T.; Kudin, K. N.; Burant, J. C.; Millam, J. M.; Iyengar, S. S.; Tomasi, J.; Barone, V.; Mennucci, B.; Cossi, M.; Scalmani, G.; Rega, N.; Petersson, G. A.; Nakatsuji, H.; Hada, M.; Ehara, M.; Toyota, K.; Fukuda, R.; Hasegawa, J.; Ishida, M.; Nakajima, T.; Honda, Y.; Kitao, O.; Nakai, H.; Klene, M.; Li, X.; Knox, J. E.; Hratchian, H. P.; Cross, J. B.; Adamo, C.; Jaramillo, J.; Gomperts, R.; Stratmann, R. E.; Yazyev, O.; Austin, A. J.; Cammi, R.; Pomelli, C.; Ochterski, J. W.; Ayala, P. Y.; Morokuma, K.; Voth, G. A.; Salvador, P.; Dannenberg, J. J.; Zakrzewski, V. G.; Dapprich, S.; Daniels, A. D.; Strain, M. C.; Farkas, O.; Malick, D. K.; Rabuck, A. D.; Raghavachari, K.; Foresman, J. B.; Ortiz, J. V.; Cui, Q.; Baboul, A. G.; Clifford, S.; Cioslowski, J.; Stefanov, B. B.; Liu, G.; Liashenko, A.; Piskorz, P.; Komaromi, I.; Martin, R. L.; Fox, D. J.; Keith, T.; Al-Laham, M. A.; Peng, C. Y.; Nanayakkara, A.; Challacombe, M.; Gill, P. M. W.; Johnson, B.; Chen, W.; Wong, M. W.; C. Gonzalez, C.; Pople, J. A. *Gaussian 03*, revision B.05; Gaussian, Inc.: Pittsburgh, PA, 2003.

(11) (a) The fraction of anion radical present as the 3:1 complex,  $\alpha_3$ , is given by<sup>11b</sup>

$$\alpha_3 = \frac{K_3 K_9 K_{10} C_{HA}^3}{1 + K_3 C_{HA} + K_3 K_9 C_{HA}^2 + K_3 K_9 K_{10} C_{HA}^3} \cong K_{10} C_{HA}$$

where the final approximation holds for the case where the 2:1 complex is dominant, i.e., the third term in the denominator is much greater than any of the other terms. Calculations using the values of  $K_3$ ,  $K_9$ , and  $K_{10}$  found in this work show that the 2:1 complex is dominant for  $C_{HA} \geq 50$  mM. Thus, the fraction of anion radical present as the 3:1 complex will increase in proportion to  $C_{HA}$ . (b) Harris, D. C. *Quantitative Chemical Analysis*, 6th ed.; Freeman: New York, 2003; pp 269–272.

(12) Izutsu, K. *Electrochemistry in Nonaqueous Solutions*; Wiley-VCH: Weinheim, 2002; pp 70–75.